Supplemental data

Supplemental Figures and Legends

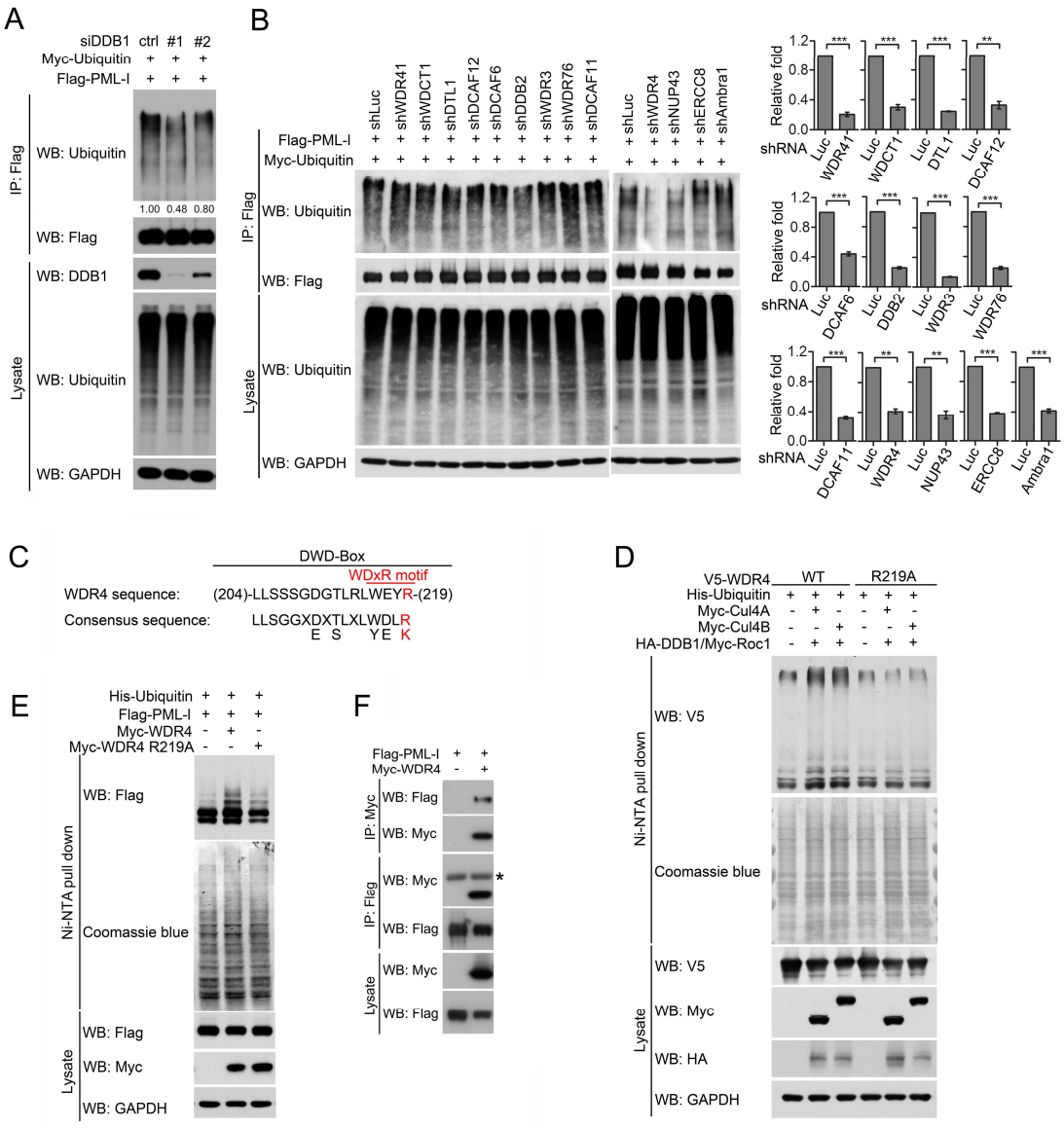

Supplemental Figure 1. WDR4 functions as a substrate adaptor of CRL4 to promote PML ubiquitination. (A, B) Immunoprecipitation analysis for PML-I ubiquitination in 293T cells transfected with indicated siRNAs or stably expressing indicated shRNAs. The relative amounts of PML-I ubiquitination is indicated in (A). The knockdown

efficiency of each DCAF shRNA was assayed by RT/qPCR analysis and shown in (B). Data are mean ± SD, n=3 per group, $**p<0.01$, $***p<0.001$, two-tailed Student's *t* test. (C) Alignment of the sequence of WDR4 amino acid 204 to 219 with the consensus sequence of DWD box. WDxR motif is indicated. (D) Ni-NTA pull down analysis for WDR4 ubiquitination in 293T cells transfected with indicated constructs. (E) Ni-NTA pull down analysis for PML-I ubiquitination in 293T cells transfected with indicated constructs. (F) Immunoprecipitation analysis of the interaction between WDR4 and PML-I in transfected 293T cells. Asterisk marks a nonspecific band.

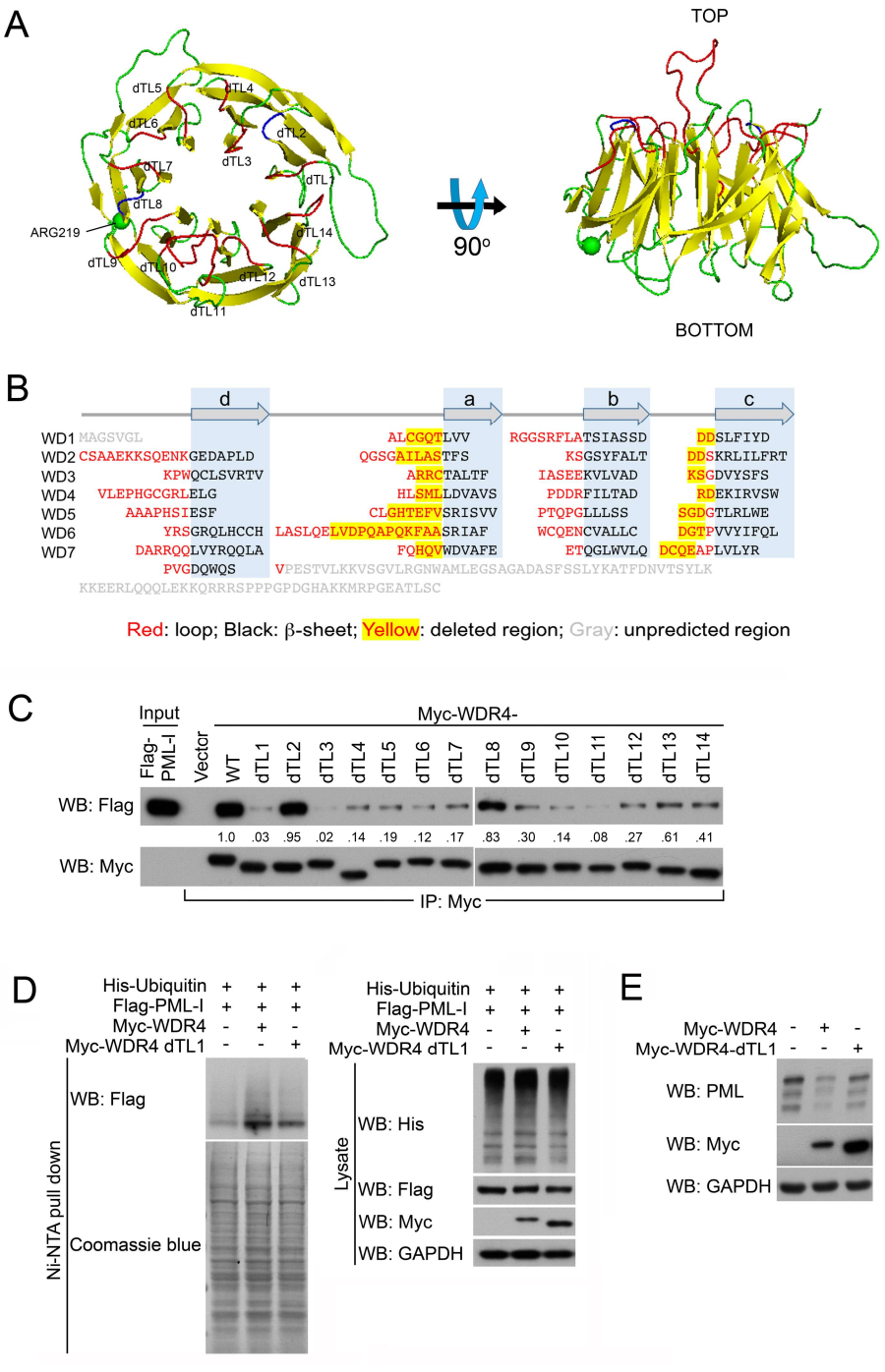

Supplemental Figure 2. Identification of the region in WDR4 responsible for PML binding, ubiquitination, and degradation. (A) Predicted structure of WD40-repeat domain of WDR4, based on the yeast Trm82 crystal structure (PDB Accession Code 2VDU). Residues that are deleted in each mutant are in red whereas other loop residues are in green. The R219 residue is marked by a green ball. (B) Amino acid

sequences of WDR4. Residues outside of the predicted structure are in gray. Residues in the β-sheet and loop are in black and red, respectively. Deleted residues are highlighted in yellow. The deletion mutants are named in order from N- to C-terminus as dTL1 to dTL14. (C) In vitro pull down analysis of WDR4 mutants bound on Myc-beads with baculovirally purified PML-I. The relative amounts of bound PML-I are indicated. (D) Immunoprecipitation analysis of PML-I ubiquitination in 293T cells transfected with indicated constructs. (E) Western blot analysis of endogenous PML in H1299 cells transfected with indicated constructs.

A

Anatomic Site		Nature	Pathology	High expression of WDR4 (ratio)
Adrenal gland		Benign	Adenoma, cortical	0/1
		Malignant	Adrenocortical carcinoma	0/1
Bladder, urinary		Malignant	Transitional cell carcinoma	0/2
Breast		Benign	Fibroadenoma	0/2
		Malignant	Invasive ductal carcinoma	0/3
Brain (cerebellum)		Benign	Meningioma, fibroblastic	0/1
		Malignant	Malignant meningioma	0/1
Brain		Benign	Meningioma, fibroblastic	0/1
		Benign	Astrocytoma	0/1
Esophagus		Malignant	Squamous cell carcinoma	3/3
Stomach		Malignant	Adenocarcinoma	1/3
Intestine	small intestine	Benign	Adenoma	0/1
		Malignant	Adenocarcinoma	0/1
	colon	Benign	Adenoma	0/1
		Malignant	Adenocarcinoma	0/3
	rectum	Malignant	Adenocarcinoma	1/3
Kidney		Malignant	Clear cell carcinoma	0/2
Liver		Malignant	Hepatocellular carcinoma	1/4
Lung		**Malignant**	**Squamous cell carcinoma**	**2/2**
		Malignant	**Adenocarcinoma**	**1/1**
		Malignant	**Small cell carcinoma**	**1/1**
Lymph node	neck	Malignant	Lymphoma, Hodgkin lymphoma	0/1
	axillary	Malignant	Lymphoma, non-Hodgkin B-cell lymphoma	0/1
	neck	Malignant	Lymphoma, anaplastic large cell lymphoma	0/1
Head and neck	salivary gland, parotid	Benign	Pleomorphic adenoma	0/1
	salivary gland	Malignant	Adenoid cystic carcinoma	0/1
	oral cavity, hard palate	Malignant	Adenocarcinoma	0/1
	oral cavity, tongue	Malignant	Squamous cell carcinoma	0/1
	nasopharynx	Malignant	Nasopharyngeal carcinoma, NPC	0/1
	nasal cavity	Malignant	Melanoma	1/1
Ovary		Benign	Granulosa cell tumor	0/1
		Malignant	Adenocarcinoma	1/1
		Malignant	Endometrioid adenocarcinoma	0/1
Prostate		Malignant	Adenocarcinoma	0/2
Skin (trunk)		Malignant	Squamous cell carcinoma	1/1
Testis		Malignant	Seminoma	0/2
Thyroid		Benign	Adenoma	1/3
		Malignant	Follicular carcinoma	0/1
		Malignant	Follicular papillary adenocarcinoma	0/1
Uterus	cervix	Malignant	Squamous cell carcinoma	1/2
	endometrium	Malignant	Adenocarcinoma	0/2

B

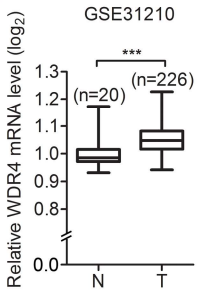

C

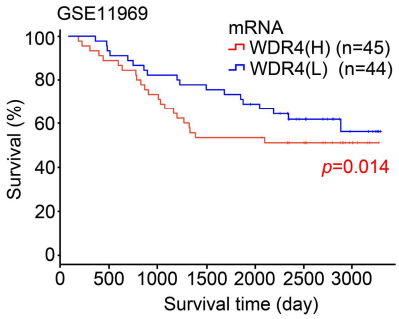

Supplemental Figure 3. WDR4 expression and its prognostic value in lung cancer. (A) Summary of the IHC data of WDR4 expression in various malignant and benign tumors. (B) *WDR4* mRNA expression profiles in non-tumor (N) and tumor (T) lung tissues (B) revealed from indicated GEO data set. Data are mean ± SD, n=20 for (N), n=226 for (T), ***p<0.001, two-tailed Student's t test. (C) Kaplan-Meier analysis of

lung cancer patient survival with *WDR4* mRNA expression profiles. Data were retrieved from indicated GEO data set. High and low expression was defined using the median expression level as a cut point. *P*-value is determined by log-rank test.

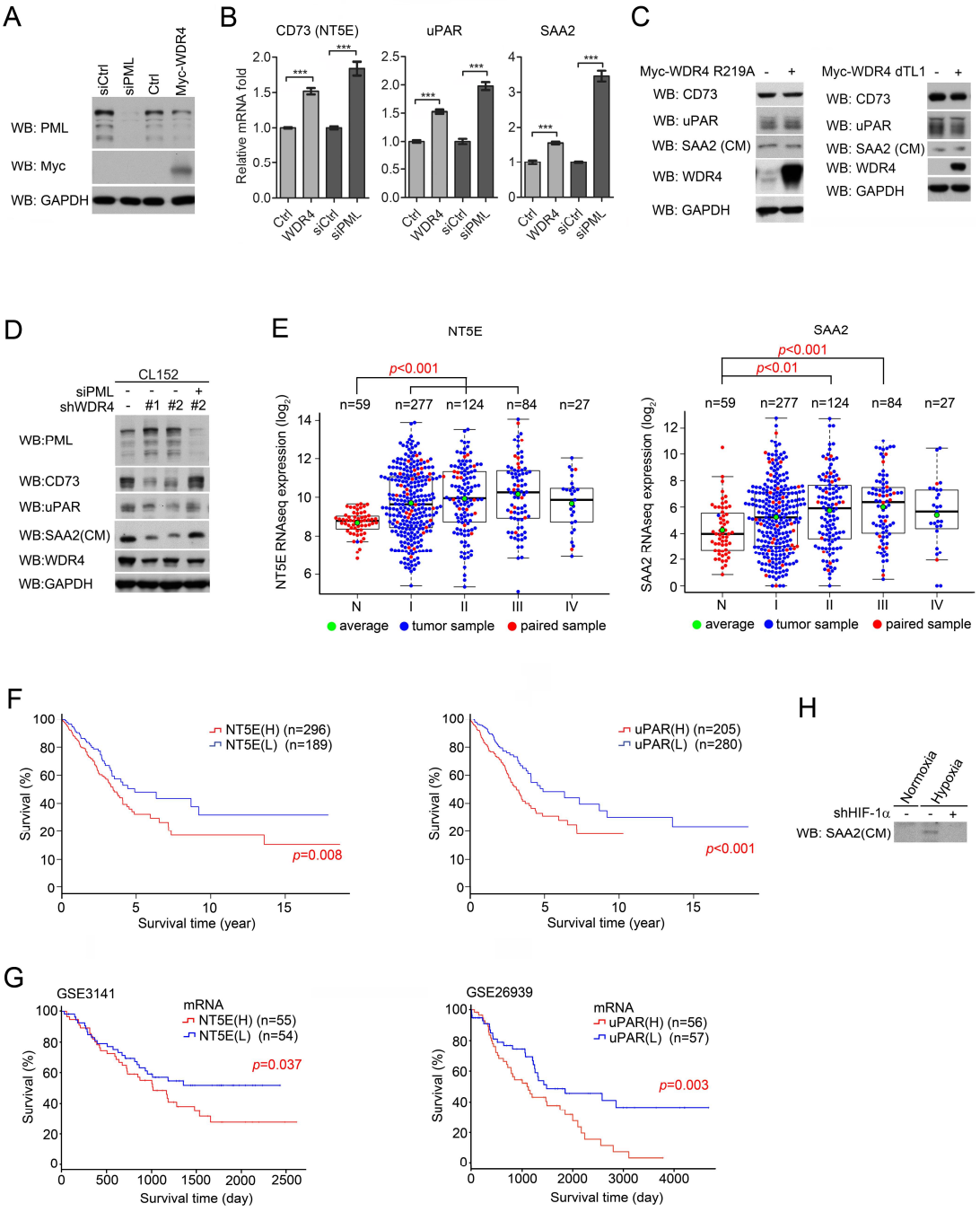

Supplemental Figure 4. WDR4/PML axis induces a number of tumor-promoting genes. (A) Western blot analysis for WDR4 and PML expression in A549 cells transfected with WDR4 construct or PML siRNA. (B) RT-qPCR analysis of the expression of indicated genes in A549 cells as in (A). Data are mean ± SD, n=3 per group, ***p<0.001, two-tailed Student's t test. (C) Western blot analysis of indicated

proteins in A549 (left) or H1299 (right) cells transfected with indicated constructs. (D) Western blot analysis of indicated proteins in CL152 cells stably expressing indicated shRNAs. (E) Expression profiles for *NT5E and SAA2* mRNA in lung adenocarcinoma tissues and adjacent normal tissues derived from TCGA data set. *P*-values are determined by one-way ANOVA with Tukey's post test. (F) Kaplan-Meier analysis of lung adenocarcinoma patient survival with the corresponding expression profiles derived from TCGA data set. High and low expression was defined using an optimized cut point. (G) Kaplan-Meier analysis of lung cancer patient survival with the corresponding expression profiles. Data were retrieved from indicated GEO data set. High and low expression was defined using the median expression level as a cut point. P-values in (F) and (G) are determined by log-rank test. (H) Western blot analysis of SAA2 in the CM of H1299 cells stably expressing control or HIF-1α shRNA and cultured in hypoxia or normoxia conditions for 24 hr. The knockdown efficiency of HIF-1α shRNA is shown in Figure 4F.

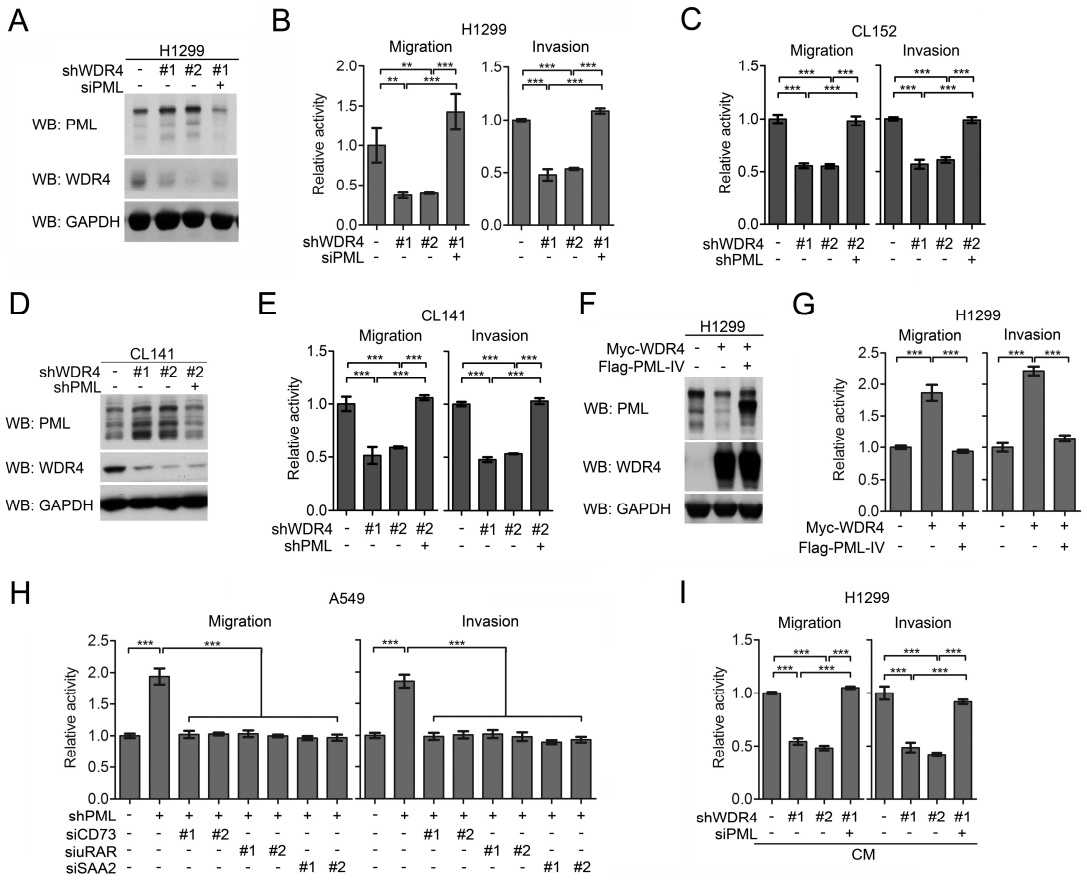

Supplemental Figure 5. WDR4/PML axis promotes lung cancer cell migration and invasion. (A) Western blot analysis of H1299 cells stably expressing WDR4 shRNA and/or PML siRNA. (B) Migration and invasion activities of cells shown in (A). (C) Migration and invasion assays of CL152 cells stably expressing indicated shRNAs. The expression levels of WDR4 and PML in these stable cells are shown in Supplemental Figure 4D. (D) Western blot analysis of CL141 cells stably expressing indicated shRNAs. (E) Migration and invasion assays of cells shown in (D). (F) Western blot analysis of H1299 cells stably expressing WDR4 and/or PML-IV. (G) Migration and invasion activities of cells shown in (F). (H) Migration and invasion activities of A549 cells stably expressing PML shRNA and transfected with indicated siRNAs. (I) Migration and invasion activities of parental H1299 cells treated with CM

derived from cells as in (A). Data shown in (B), (C), (E), (G), (H) and (I) are mean ± SD, n=3 per group, **p<0.01, ***p<0.001, one-way ANOVA with Tukey's post test.

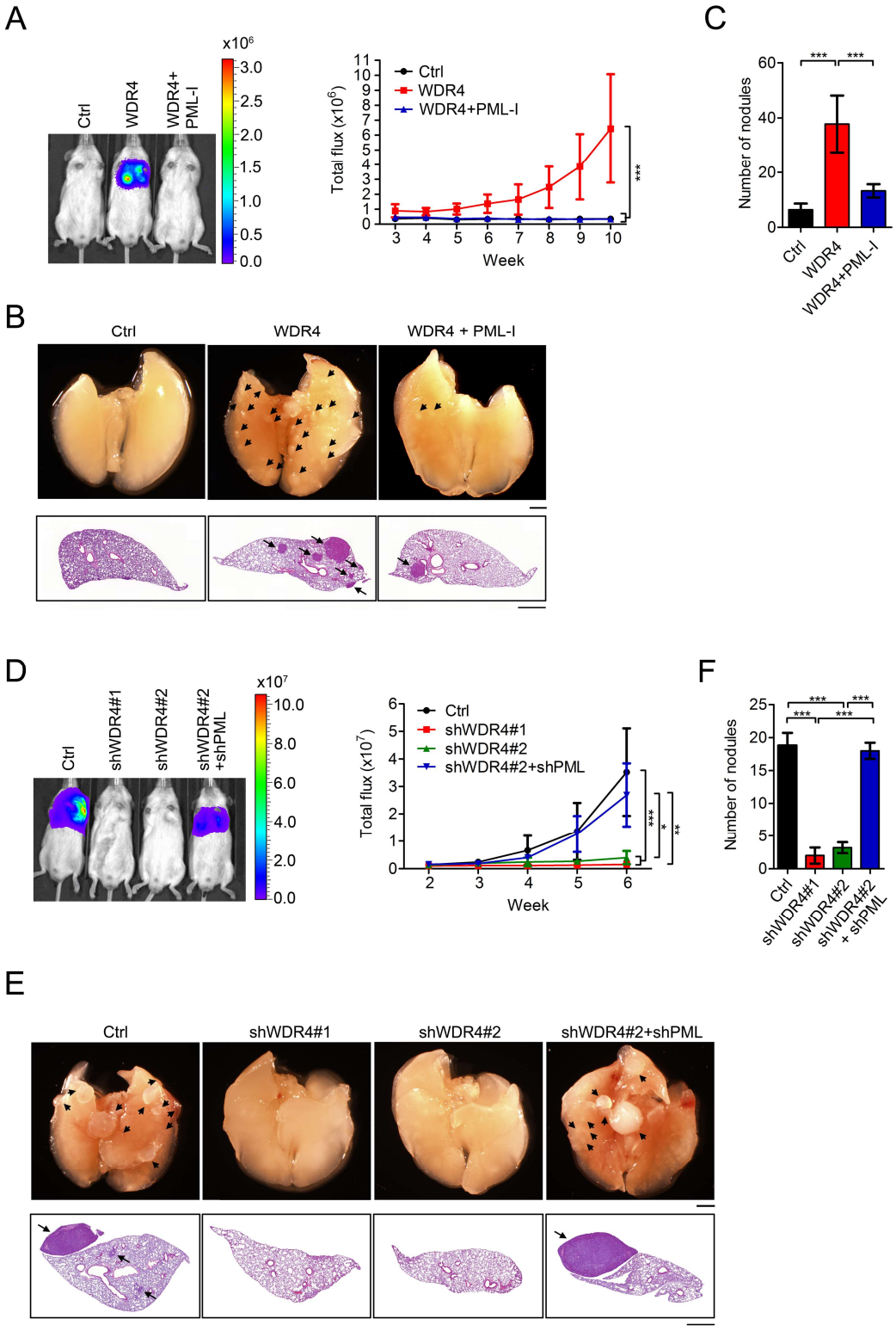

Supplemental Figure 6. WDR4/PML axis promotes lung cancer metastasis. (A) Bioluminescence analysis of lung metastasis derived from indicated A549 cells

(established in Figure 5E). Representative images at week 10 (left) and kinetics of metastasis at indicated time points (right) are shown. Data are mean ± SD, n=8 per group, ***p<0.001 for week 10 data, one-way ANOVA with Tukey's post test. (B) Lung metastasis and histological analysis of the lung at week 10. Nodules are indicated by arrows. Bars, 2 mm (top) and 500 μm (bottom). (C) Number of metastatic nodules at the surface of lung at week 10. Data are mean ± SD, n=8 per group, ***p<0.001, one-way ANOVA with Tukey's post test. (D) Bioluminescence analysis of lung metastasis derived from indicated CL152 cells (established in Supplemental Figure 4D). Representative images at week 6 (left) and kinetics of metastasis at indicated time points (right) are shown. Data are mean ± SD, n=5 per group, *p<0.05, **p<0.01, ***p<0.001 for week 6 data, one-way ANOVA with Tukey's post test. (E) Lung metastasis and histological analysis of the lung at week 6. Nodules are indicated by arrows. Bars, 2 mm (top) and 500 μm (bottom). (F) Number of metastatic nodules at the surface of lung at week 6. Data are mean ± SD, n=5 per group, ***p<0.001, one-way ANOVA with Tukey's post test.

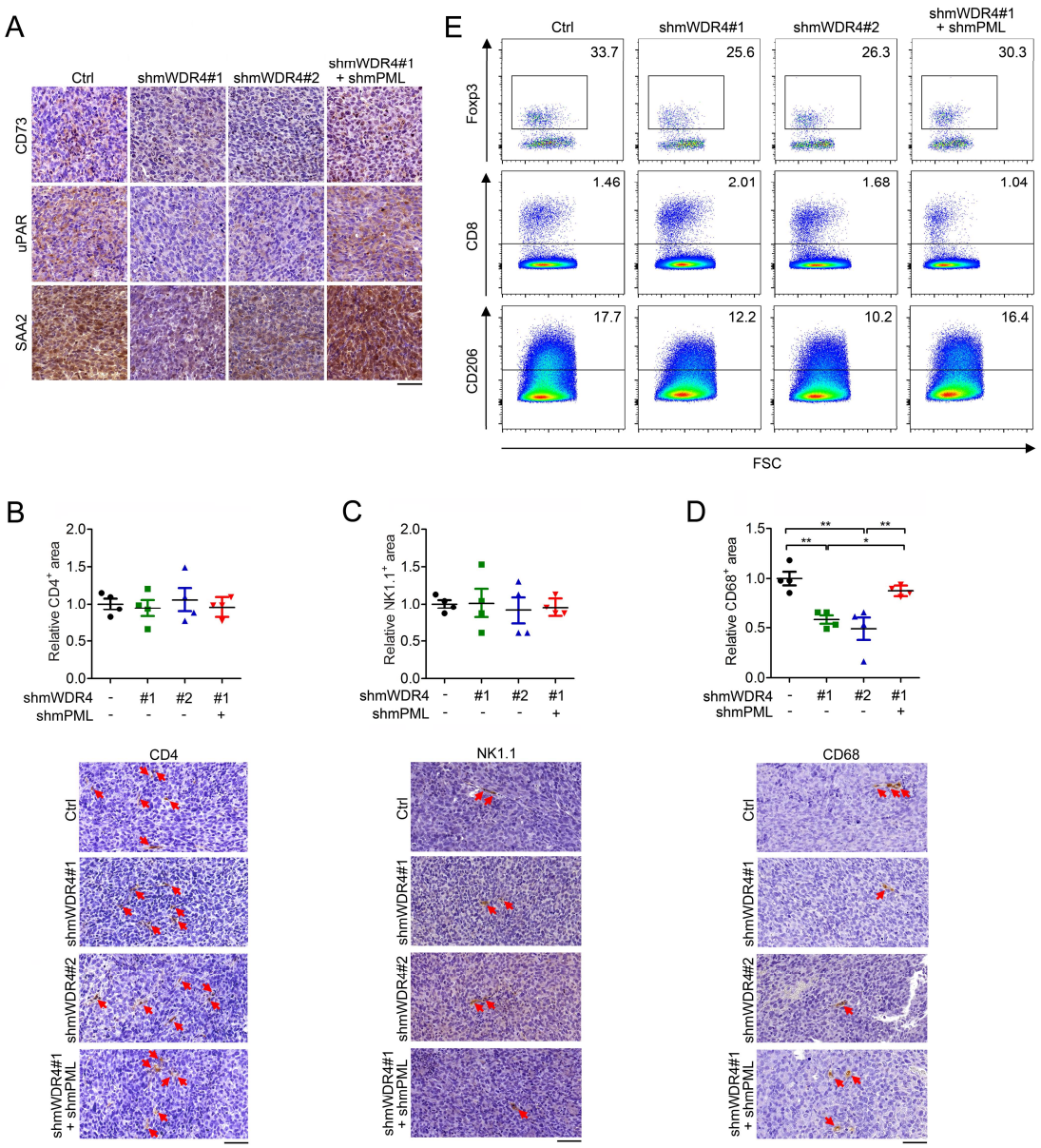

Supplemental Figure 7. The roles of WDR4/PML axis in regulating downstream effectors and intratumoral immune cells in a syngeneic mouse model. (A) IHC staining for the expression of CD73, uPAR, and SAA2 in primary tumors derived from indicated LLC1 xenografts. Bar, 50 μm. (B, C, D) IHC analyses of CD4, NK1.1, and CD68 using primary tumors at the time of harvest. Quantitative data are shown on the top and representative images are on the bottom. Cells stained positive are indicated by arrows. Data are mean ± SD, n=4 per group, *p<0.05, **p<0.01, one-

way ANOVA with Tukey's post test. Bar, 50 μm. (E) Representative flow cytometry data for $CD4^+Foxp3^+$ Tregs, $CD8^+$ T cells, and $CD68^+CD206^+$ M2-like macrophages in the primary tumors generated by inoculating LLC1 derivatives in syngeneic mice. In all experiments, cells were first gated on $CD45^+$ population and then on $CD4^+$ population (top) or $CD68^+$ population (bottom).

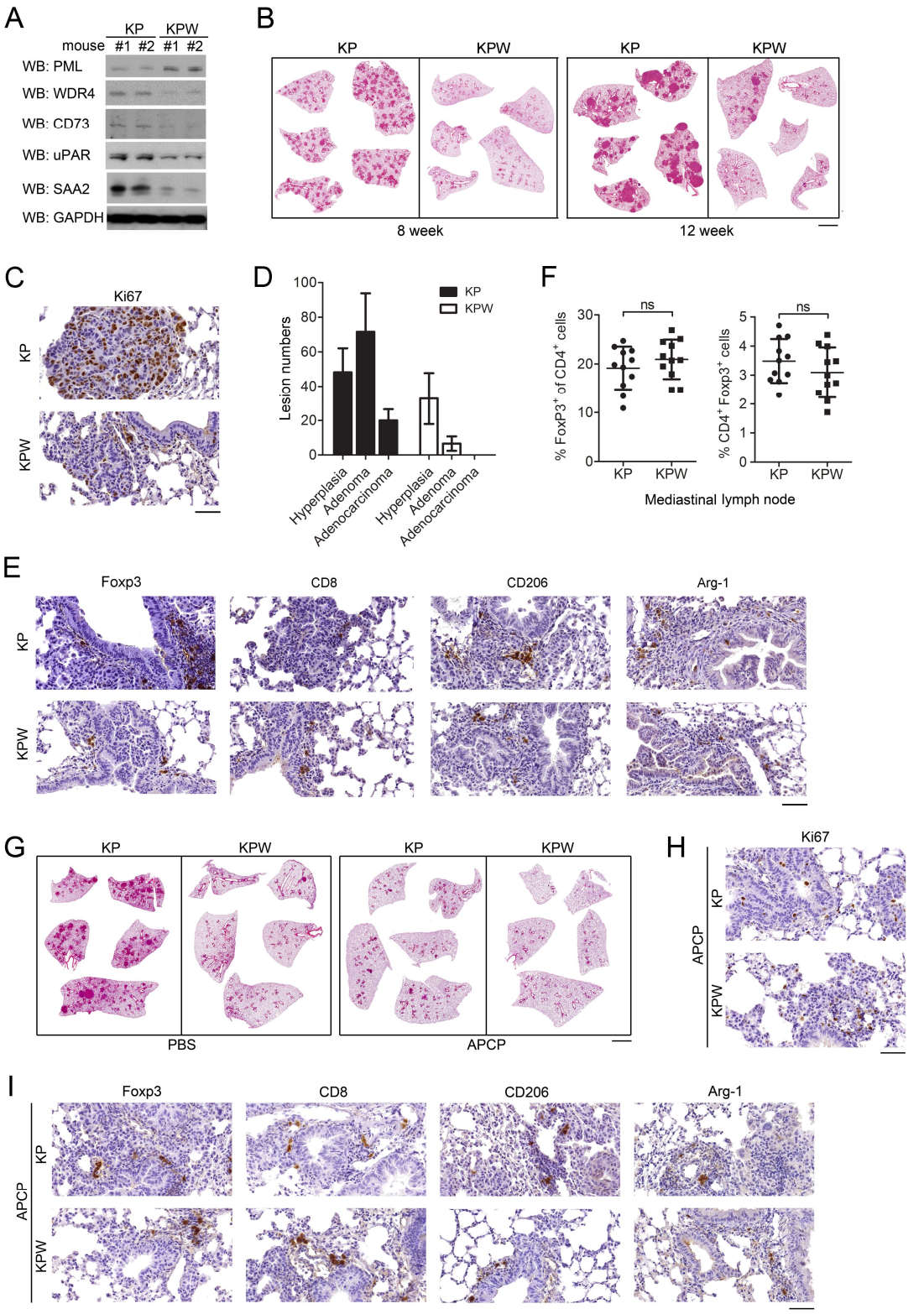

Supplemental Figure 8. Lung tumorigenesis and intratumoral immune cells in KP and KPW mice. (A) Western blot analysis of the expression of indicated proteins in lung

tumors derived from KP and KPW mice. (B) Histological lung sections of KP and KPW mice at 8 and 12 weeks after Ad-Cre administration. Bar, 2 mm. (C, E) Representative images for IHC data of Ki67, Foxp3, CD8, CD206 and Arg-1 in the lung tumors of KP and KPW mice at 8 weeks after tumor induction. Bar, 50 μm. (D) Numbers of hyperplastic lesions, adenomas and adenocarcinomas in KP and KPW mice at 8 weeks after Ad-Cre administration. Data are mean ± SD, n=5 per group. (F) Mediastinal lymph nodes were isolated from KP and KPW mice at 8 weeks after Ad-Cre administration and analyzed for Tregs by flow cytometry as in Figure 9F. The percentages of $Foxp3^+$ cells among $CD4^+$ T cells and $CD4^+Foxp3^+$ cells among total analyzed lung cells are quantified. Data are mean ± SD, n=11, two-tailed Student's *t* test. (G) Histological lung sections of APCP-treated or untreated KP and KPW mice at 8 weeks after Ad-Cre administration. Bar, 2 mm. (H, I) Representative images for IHC data of Ki67, Foxp3, CD8, CD206 and Arg-1 in lung tumors of APCP-treated KP and KPW mice at 8 weeks after tumor induction. Bar, 50 μm.

Supplemental Tables

Supplemental Table 1: Information for antibodies used in this study

Protein	Assay	Antibody
WDR4 (human)	WB, IP	ab169526, Abcam
	IHC	ab56765, Abcam
Flag	WB	F3165, Sigma
His	WB	631212, Clontech
GAPDH	WB	GTX100118, GeneTex
Myc	WB	9E10, Santa Cruz
HA	WB	H9658, Sigma
V5	WB	AB3792, Millipoare
Rabbit IgG	IP	ab46540, Abcam
PML (human)	WB, IP	NB100-59787, Novus
	IHC	PG-M3, Santa Cruz
PML (mouse)	WB	05-718, Millipore
CD73 (human)	WB	ab137595, Abcam
CD73 (mouse)	IHC	ab175396, Abcam
SAA2	WB	ab125414, Abcam
uPAR (human)	WB	SAB2700745, Sigma
uPAR (mouse)	WB, IHC	ab103791, Abcam
HIF-1α	WB	ab2185, Abcam
DDB1	WB	ab21080, Abcam
Roc1	WB	ab2977, Abcam
Cul4A	WB	C0371, Sigma
Cul4B	WB	C9995, Sigma
Cul1	WB	sc-11384, Santa Cruz
Cul2	WB	sc-10781, Santa Cruz
Cul3	WB	sc-166054, Santa Cruz
Cul5	WB	sc-13014, Santa Cruz

ubiquitin	WB	3936, Cell Signaling
Arginase1	IHC	sc-20150, Santa Cruz
Ki67	IHC	ab16667, Abcam
NK1.1	IHC	ab197979, Abcam
CD8	IHC	14-0808, eBioscience
	FC	17-0081, eBioscience
CD206	IHC	MCA2235, AbD Serotec
	FC	141729, Biolegend
CD68	IHC	MCA1957GA, AbD Serotec
	FC	137017, Biolegend
Foxp3	IHC	14-5773, eBioscience
	FC	12-5773, eBioscience
CD4	IHC	sc-13573, Santa Cruz
	FC	11-0042, eBioscience
CD25	FC	17-0251, eBioscience
CD45	FC	103140, Biolegend
CD16/CD32	Blocking	14-0161, eBioscience

Supplemental Table 2: Primers for quantitative PCR and mouse genotyping

Assay	Gene name		Sequence (5' to 3')
Quantitative PCR	CD73	F	AGGCCAAATTTCCAATTCTGAGTG
		R	TGAGAGAAAAGGGGTTTCTTTGGA
	uPAR	F	AAGCTATATGGTAAGAGGCTGTGC
		R	CCACTTTTAGTACAGCAGGAGACA
	SAA2	F	GCTCAGACAAATACTTCCATGCTC
		R	AGTCTCTGGATATTCTCTCTGGCA
	WDR76	F	GTATTTTATCACTGCCGGATTGAGG
		R	TCAGTCAAAGAAATCAAAGGCTGAC
	NUP43	F	AGCTAATGTTCACCAGTCTGTCAT
		R	AAGTGTTCACAGACAGAGACCTAC
	DCAF11	F	TGAGATCAAGACACAAGTGGAACT
		R	AGATCATTGGGCAAGAAGTGAGAT

	WDR4	F	GAGAGCACCGTGTTAAAGAAAGTC
		R	CTGCAGTCTCTCCTCTTTCTTCTT
	WDR3	F	GACAGAGTTGTAAACCTTGCAGTC
		R	TTAACCTCAGGATCTTCCTCCTCT
	WDR41	F	TGTACGCATTTGGGAGTTAAGAGA
		R	TGTACGCATTTGGGAGTTAAGAGA
	DDB2	F	ACCCTCTCAATACCAACCAGTTTT
		R	ACAAAACCAGATGTTGATGGTGTC
	ERCC8	F	TTCTCACATTCTACAGGGTCACAG
		R	TCAAACATCCTGATGCTCTTCTCA
	DCAF12	F	TCTCAGTGGTTGAATCATAGGCAA
		R	TTTCAGAATGGGGATCTTGGTGAT
	WDTC1	F	TCCATAACCACAGAAAGAGCATGA
		R	CACTCTCAAACGGTTGTTGTAGTC
	DTL1	F	AGGAGAAACCAGGAGGTGATAAAC
		R	GAGTACTCTGGCTACTCGTTACTG
	DCAF6	F	CAATTTCTGGGGTGCTAACTTTGT
		R	TAAAATTGGGTCAAACGGATGTGG
	Ambra1	F	CCACTTGGACACTACTTACTCACA
		R	CTGTTCCATCTATGGGGATCTCTG
	β-actin	F	CATGTACGTTGCTATCCAGGC
		R	CTCCTTAATGTCACGCACGAT
	GAPDH	F	TGTTGCCATCAATGACCCCTT
		R	CTCCACGACGTACTCAGCG
Genotyping	Kras	y116	TCCGAATTCAGT GACTACAGATG
		y117	CTAGCCACCATGGCTTGAGT
		y118	ATGTCTTTCCCCAGCACAGT
	p53	T008	CACAAAAACAGGTTAAACCCAG
		T009	AGCACATAGGAGGCAGAGAC
	WDR4	F7016	TGGAGCTCACGGGGGCAGGTGAGAC
		F7195	TCCATGGTTATAAATCGCCATGTAG
		F11155	AAGGAGGGTTTATTCTGGCTGGTCG
		F13575	TCCATGGCAGCTGAGAATATTGTAG

Supplemental Table 3: Targeting sequences for siRNAs and shRNAs

Gene name	Type	Target sequence (5' to 3')
PML (human)	shRNA	CACCCGCAAGACCAACAACAT
PML (mouse)	shRNA	GCACAGATGTGCTCAGCTATA
WDR4 (human)	shRNA#1	GCACCGTGTTAAAGAAAGTCT
	shRNA#2	AGAGTTTGTGAGCCGTATCTC
WDR4 (mouse)	shRNA#1	CCGCATAGCATCGAGTCTTTC
	shRNA#2	ATGACAGTAAGCGTCTGATTC
ERCC8	shRNA	GCGCTAATGCTTGAACTCTTT
DDB2	shRNA	GCTGAAGTTTAACCCTCTCAA
DTL	shRNA	GCCTAGTAACAGTAACGAGTA
DCAF6	shRNA	CTGAACAATTTCTTCAGCCTT
NUP43	shRNA	GACCATCAGTTATTGTGTGAT
DCAF11	shRNA	CCGTAAATTCAAGAGCATCAA
WDTC1	shRNA	CGCATGATCCATAACCACAGA
DCAF12	shRNA	CATGATGAAACCTGGAGGAAT
WDR76	shRNA	CTGTCTAAGGAGCCTAGTAAT
WDR41	shRNA	TATACCTTGCTGTCTAGTTTA
WDR3	shRNA	CCTGGAATACAAGATACTCTT
Ambra1	shRNA	GCATGTGGACTCTTAACTGTA
HIF1-α	shRNA	CCAGTTATGATTGTGAAGTTA
DDB1	siRNA#1	CACUAGAUCGCGAUAAUAA
	siRNA#2	CAUCUCGGCUCGUAUCUUG
WDR4	siRNA#1	GGACGUGGCUUUCGAGGAG
	siRNA#2	GCAGACAGCAGUUGGUGUA
PML	siRNA	GAGCUCAAGUGCGACAUCA
CD73	siRNA#1	GCAAAUACCUAGGCUAUCU
	siRNA#2	GUAGUCAAAUUAGAUGUUC
uPAR	siRNA#1	CGGACUGGCUUGAAGAUCA
	siRNA#2	CGAGGUUGUGUGUGGGUUA
SAA2	siRNA#1	CCGAUCAGGCUGCCAAUAA
	siRNA#2	GGACAUGUGGAGAGCCUAC

Supplemental Table 4: Clinical pathological characteristics of lung cancer patients

Clinical parameters		Total patients	PML protein expression				WDR4 protein expression			
		120	H (N=42)	%	L (N=78)	%	H (N=30)	%	L (N=90)	%
Age	<65	56	19	33.9	37	66.1	17	30.9	38	69.1
	≧ 65	64	22	34.4	42	65.6	13	20.3	51	79.7
Sex	Male	61	25	41.0	36	59.0	18	29.5	43	70.5
	Female	59	16	27.1	43	72.9	12	20.7	46	79.3
Smoker	Yes	39	16	41.0	23	59.0	11	28.2	28	71.8
	No	68	18	26.5	50	73.5	13	19.4	54	80.6
Stage	I-II	77	26	33.8	51	66.2	19	25.0	57	75.0
	III-IV	43	15	34.9	28	65.1	11	25.6	32	74.4
Type	ADC	92	30	32.6	62	67.4	25	26.3	70	73.7
	SCC	19	6	31.6	13	68.4	5	26.3	14	73.7
T stage	I-II	102	36	35.3	66	64.7	25	24.8	76	75.2
	III-IV	17	4	23.5	13	76.5	5	29.4	12	70.6
N stage	0	77	27	35.1	50	64.9	20	26.3	56	73.7
	1-2	43	14	32.6	29	67.4	10	23.3	33	76.7
M stage	0	110	39	35.5	71	64.5	28	25.7	81	74.3
	1	9	2	22.2	7	77.8	2	22.2	7	77.8
WDR4	-	30	20	66.7	10	33.3	-	-	-	-
	+	90	22	24.4	68	75.6	-	-	-	-

***p<0.001, Fisher's exact test